Study of transport properties and electronic structure of the $Co_{1-x}Rh_xSb_3$ skutterudite

K. Wojciechowski[1], J. Tobola[2], J. Leszczynski[1], S. Kaprzyk[2], A. Malecki[1]
[1]Faculty of Materials Science and Ceramics
[2]Faculty of Physics and Nuclear Techniques
AGH University of Science and Technology
Al. Mickiewicza 30, 30-059 Cracow, Poland
e-mail: gcwojcie@cyf-kr.edu.pl. tel.: (+48)12-617-34-42, fax: (+48)12-617-24-93

Abstract

Physical properties of $CoSb_3$-$RhSb_3$ pseudo-binary system were investigated both experimentally and theoretically. The analysis of the X-ray diffraction data using the Rietveld method showed that the system can form solid solution of the skutterudite structure at high temperatures in the whole range of composition. Electrical conductivity and thermopower were studied in the temperature range of 300 – 570 K. Furthermore, Hall coefficient measurements at room temperature allowed estimating of effective masses of carriers. The electronic structure of $Co_{1-x}Rh_xSb_3$ was calculated using the KKR-CPA method within the LDA approach. The dispersion curves for $CoSb_3$ and $RhSb_3$ end-point compounds as well as density of states for $Co_{1-x}Rh_xSb_3$ (x = 0.25, 0.5, 0.75) alloys were deduced from our computations.

Introduction

The formation of solid solutions of isostructural compounds is one of techniques used in order to improve thermoelectric figure of merit by reducing lattice thermal conductivity. In case of thermoelectric materials belonging to the skutterudite group some of compositions form full range solid solutions, such as CoP_3-$CoAs_3$ [1-2], $RhSb_3$-$IrSb_3$ [3,4]. There are also known partial solid solutions in similar systems: $CoAs_3$-$CoSb_3$ [1], $CoSb_3$-$IrSb_3$ [5]. It was demonstrated [4] that alloying in these systems can result in reduction in thermal conductivity by a factor of 2-3 times. On the other hand, e.g. in case of $IrSb_3$ – $RhSb_3$ solid solution, only a small effect of alloying on the electronic properties (conductivity and Seebeck coefficient) were measured and in consequence significant increase of ZT parameter over the values determined for $IrSb_3$ was observed.

Both $CoSb_3$ and $RhSb_3$ isostructural compounds have different lattice constants of about 20% but their physical poperties are quite similiar (Table 1). It permits to expect that both compounds should form solid solutions either in the whole range of compositions or with relatively narrow miscibility gap. Although detailed experimental data for both $CoSb_3$ and $RhSb_3$ are available [6-19], a thorough characterization of their alloys has been not accomplished up to now to our best knowledge. Therefore, the aim of this work was to make systematic studies of the $CoSb_3$-$RhSb_3$ system in the full range of compositions in order to determine the solubility range and influence of alloying on both thermal and electrical transport properties. Moreover, electronic band structure calculations were performed for selected compositions.

Table 1. Some properties of $CoSb_3$ and $RhSb_3$ with skutterudite structure (sp.g. Im3) at room temperature.

Property	$CoSb_3$	$RhSb_3$
Cell size *a*	9.0385 Å [22]	9.2322 Å [8]
X-ray density	7.63 gcm^{-3} [22]	7.90 gcm^{-3} [8]
Peritectic decomposition temp.	873 °C [14]	900 °C [14]
Band gap E_g (experimental)	0.55 eV [9] (transport) 0.07 eV [12] (optical)	-
Band gap E_g (theoretical)	0.14 eV [13]	semimetal [11, 13, 19]
Hall mobility	e = 72 $cm^2V^{-1}s^{-1}$ [20] p=3.4 $\cdot 10^3$ $cm^2V^{-1}s^{-1}$ [15]	p=8 $\cdot 10^3$ $cm^2V^{-1}s^{-1}$ [15] p=1$\cdot 10^3$ $cm^2V^{-1}s^{-1}$ [7]
Hall concentration	$e = 6.1 \cdot 10^{17}$ [20] p= 4 $\cdot 10^{17}$ [15]	p= 3.5 $\cdot 10^{18}$ [15] p= 1 $\cdot 10^{19}$ [7]
Seebeck coefficient	-430 (*n*) [9] 142 (*p*) [13]	80 (*p*) [13]
Thermal conductivity	8.5 $Wm^{-1}K^{-1}$ [7]	10.7 $Wm^{-1}K^{-1}$ [7]
Electrical conductivity	7.0 *10^3 S m^{-1} [9]	5$\cdot 10^4$ S m^{-1} [7]
Thermal expansion coeff.	13.5 $\cdot 10^{-6}$ K^{-1} [15]	12.7 $\cdot 10^{-6}$ K^{-1} [15]
Binding energy	1.2 eV [21]	2.4 eV [21]
Transverse sound velocity	2788 m/s [20]	-
Longitudinal sound velocity	4623 m/s [20]	-
Debye temperature (K)	321 K [20]	-

Experimental

Materials were prepared by direct reaction of elements: cobalt (99.9%), rhodium (99.9%) and antimony (99.999%), The powders were mixed in stoichiometric proportions and ground with ethanol added to prevent oxidation. Dried samples were placed in the quartz crucibles and annealed for 2 hours at 400°C in the atmosphere of 10% H_2 and 90% Ar to reduce oxides on the metals surfaces. Then the powders were closed in sealed quartz ampoules coated with graphite, and annealed at 700°C for 150 hours. The resulting materials were ground and hot pressed in graphite dies (argon atmosphere, t = 20 min, p = 30 MPa, T = 770 °C) and slowly cooled down with rate of 5 °C/min to the room temperature in order to avoid fracturing. The samples of 10 mm in diameter and 20 mm in height, were cut with a diamond saw and polished.

The prepared materials were characterised by X-ray diffractometry (XRD-7 Seifert, Ni filtered CuK_α radiation) and scanning electron microscopy (JEOL JSM-840 with an electron-probe microanalysis apparatus (EPMA)). The lattice parameters were calculated from the experimental X-ray patterns using FullProf [24] refinement program implementing

Rietveld method. Mass densities were determined using the immersion technique with water as the liquid.

The electrical and thermal transport properties were measured over the temperature range from 300 to 560K. The electrical conductivity was determined by four probe AC technique. The Seebeck coefficient and thermal conductivity measurements were conducted in radiation-shielded vacuum probe by forcing variable heat flux across the sample and measuring corresponding linear variations of temperature differences and thermoelectric voltage in steady-state conditions.

The Hall coefficient R_H was measured using low frequency (7 Hz) AC sample current of 50 to100 mA/mm^2 in a constant magnetic field of 0.705 T at the room temperature. Carrier concentrations were calculated from the Hall coefficient R_H, assuming a Hall scattering factor equal to 1.0.

Structural and microstructural analysis

Microscopic observations of the samples revealed that the resulting materials had an uniform microstructure. The samples contained well-formed grains with sizes ranging from 2 to 10 μm. The measured densities were found to be from 98.0 to 99.8% of the theoretical value. XRD diffraction patterns of alloys corresponding to skutterudite structure exhibit systematic shift in positions of reflections according to composition variation (Fig. 1). Only in case of $Co_{0.83}Rh_{017}Sb_3$ a slight splitting of main reflections, with formation of lower satellite peaks on both sides of these main reflections, was observed. It may indicate an appearance of limited miscibility range close to this composition, as already noted by Fleurial *et al.* [25].

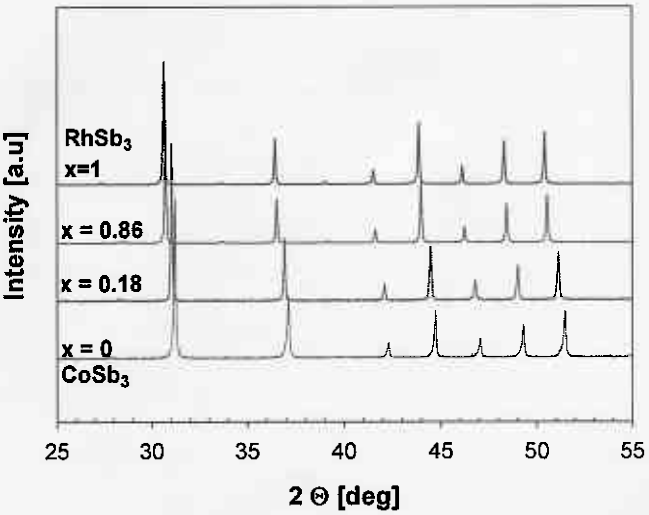

Fig. 1 Evolutional changes of XRD patterns for solid solutions of $RhSb_3$ and $CoSb_3$ isostructural compounds.

The Rietveld method was used for refining structural parameters: the lattice parameter a, and fractional coordinates of antimony position y_{Sb} and z_{Sb}. The calculations for solid solutions were made for 14 refined parameters considering pseudo-Voigt profile function and without including preferred crystal orientation and surface roughness model. Only in case of XRD patterns with split reflections more extended model, taking into account an occurrence of two additional skutterudite phases with slightly altered lattice parameters, was used. Analysis of refinement results shows that the lattice constant a changes almost linearly with the molar composition following Vegard's rule. In case of fractional coordinates of antimony position z_{Sb} and y_{Sb} only slight deviations from linear dependency can be noticed in the region close to x = 0.2.

One may conclude that $Co_{1-x}Rh_xSb_3$ alloys can form full range solid solution in high temperatures and a range of limited miscibility can exist at lower temperatures. In result, chemical and microstructural composition of samples will be dependent on cooling rate of samples after temperature treatment. However, more detailed analysis including thermal analysis DSC/DTA and structural investigations using TEM technique is required for precise characterisation of the miscibility gap.

Electrical properties

Measured room temperature electrical conductivities of undoped $CoSb_3$ and $RhSb_3$ are about $4 \cdot 10^3$ Sm^{-1} and $1.64 \cdot 10^5$ Sm^{-1} respectively, comparable to values for polycrystalline samples reported by others (Table 1). For alloys ranging from 0.1 to 0.5 the decrease of conductivity, almost one order below a value measured for pure $CoSb_3$, is noticed (Fig. 2). Such large decrease can indicate on enhanced scattering caused by micro-structural defects and strains in the range of miscibility gap rather than on scattering induced by chemical disorder in Co/Rh sublattice.

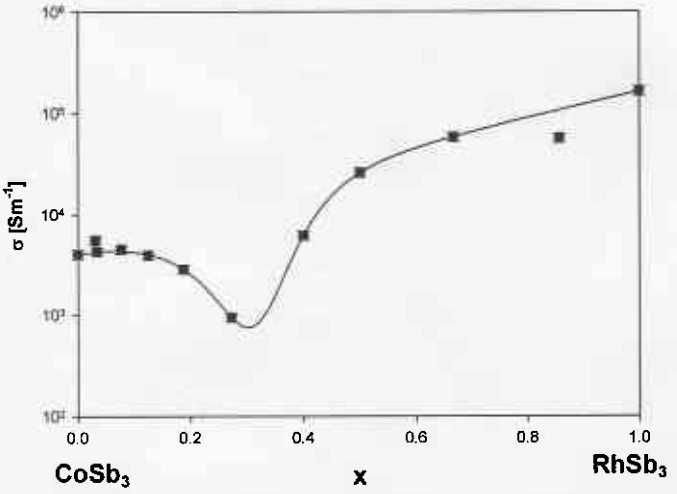

Fig. 2. Electrical conductivity σ versus molar composition at room temperature. Solid line – guide to the eye.

From temperature dependences of electrical conductivity for selected compositions (not presented) one observes semiconducting behaviour for $CoSb_3$ and its alloys with content of Rh below x<0.5. Samples with larger amount of rhodium exhibit semimetallic properties. Unexpectedly, the transition from semiconducting to semimetallic dependence does not have a monotonous character. Estimated, on basis of

temperature dependence of electrical conductivity, values of E_g systematically increase from 0.05 to 0.2 eV (for x from 0 to 0.27 respectively) and then fall to values close to 0. Calculations of density of states (DOS) curves for this system, detailed in the next part of the paper, show that band gap E_g vanishes gradually when composition changes from $CoSb_3$ to $RhSb_3$. Therefore, it seems that specific behaviour should be rather attributed to complex transport processes of carriers in the miscibility gap and experimentally estimated values of E_g include contribution of other thermally activated mechanisms.

Measurements of Seebeck coefficient were made for all samples in the temperature range from 300K to 560 K. The absolute value of the Seebeck coefficient at room temperature is the highest for pure $CoSb_3$ (-450 μVK^{-1}). Absolute values of α decrease with the increase of rhodium content. It can be also observed that the x = 0.27 sample has negative values of the Seebeck coefficient at low temperatures, while the sign turns to positive in higher temperature range. This would indicate that the character of carriers has changed with the increase of temperature. Samples with higher Rh contents exhibit positive values of thermopower. The sample of pure $RhSb_3$ has almost constant value of $\alpha = 28$ μVK^{-1} in the whole range of investigated temperatures.

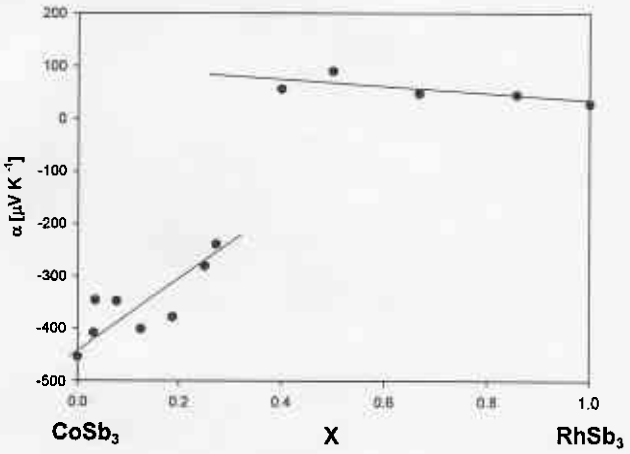

Fig 3. Seebeck coefficient α versus molar composition at room temperature. Solid lines – guide to the eye.

Table2. Selected properties of $Co_{1-x}Rh_xSb_3$ samples at room temperature.

x	carrier concentration [cm^{-3}]	mobility [$cm^2V^{-1}s^{-1}$]	Effective mass m*
0 ($CoSb_3$)	$n = 3.2 \cdot 10^{18}$	78.1	2.2
0.03	$n = 3.6 \cdot 10^{18}$	97.4	1.6
0.034	$n = 4.2 \cdot 10^{18}$	62.5	1.2
0.125	$n = 3.3 \cdot 10^{18}$	74.0	1.5
0.188	$n = 6.8 \cdot 10^{18}$	26.2	2.1
0.27	$p = 5.3 \cdot 10^{17}$	112	0.12
0.4	$p = 1.0 \cdot 10^{18}$	386	0.03
0.5	$p = 2.2 \cdot 10^{18}$	748	0.08
0.67	$p = 2.8 \cdot 10^{19}$	129	0.22
0.86	$p = 1.3 \cdot 10^{19}$	271	0.12
1 ($RhSb_3$)	$p = 1.6 \cdot 10^{19}$	925	0.09

The Hall concentration measurement results (Table 2.) remain consistent with the Seebeck coefficient data. Only for the x=0.27 sample the sign of Hall coefficient is opposite to the thermopower value. The sample belongs to the transition range where concentration of electrons and holes is comparable. This is confirmed by low value of majority carriers ($5.3 \cdot 10^{17}$ [cm^{-3}]). Therefore, the type of conductivity obtained experimentally will be strongly dependent on temperature dependence of carriers' equilibrium.

Effective mass of carriers m^* were estimated using the Seebeck coefficient and Hall carrier concentration data assuming a single parabolic band model with acoustic phonon scattering as a predominant carrier scattering mechanism (equations Eq.1 and Eq. 2):

$$S = -\frac{k_B}{e}\left(\frac{2F_1(\eta)}{F_0(\eta)} - \eta\right) \qquad \text{(Eq.1)}$$

$$n = 4\pi\left(\frac{2m^* k_B T}{h^2}\right)^{3/2} F_{1/2}(\eta) \qquad \text{(Eq.2)}$$

where: k_B is the Boltzmann's constant, η - reduced Fermi energy, F_x – the Fermi integral of order x, m^* - the effective mass and T- the absolute temperature.

Calculated effective masses of holes are comparable to masses of carriers in both pure $CoSb_3$ [9] and $RhSb_3$. Mass of electrons in n-type samples is comparable to heavy mass of carriers measured in pure $CoSb_3$. Mobility of carriers decreases for compositions close to the miscibility gap region.

Observed similarities of carriers' properties demonstrate that electronic structure of alloys should not vary significantly from the structure of their parent compounds and received materials in the whole range of composition inherit their core properties.

Thermal conductivity properties

Both polycrystalline $RhSb_3$ and $CoSb_3$ samples have similar thermal conductivity close to 10 $Wm^{-1}K^{-1}$ at room temperature comparable to values reported elsewhere (Table 1). In case of $CoSb_3$ conductivity slightly decreases with temperature; conductivity of $RhSb_3$ exhibits almost temperature independent value (Fig.4). In result of alloying of both compounds thermal conductivity significantly drops especially in the region of compositions for x from 0.1 to 0.5. The decrease corresponds to the reduction of electrical conductivity in this range. Estimated by us on basis Wiedemann-Franz law electronic contribution of thermal conductivity λ_{el} is less than 5 % in this region. Therefore, the decrease of the total thermal conductivity λ cannot be clarified exclusively by relative changes in electronic contribution and would be explained rather by scattering on mass and volume fluctuations or, consistently like in the case of electrical conductivity, by scattering caused by defects and strains in the miscibility gap.

However, detailed structural and microstructural analysis of samples for this range of compositions should provide unambiguous data helpful to clarify this point.

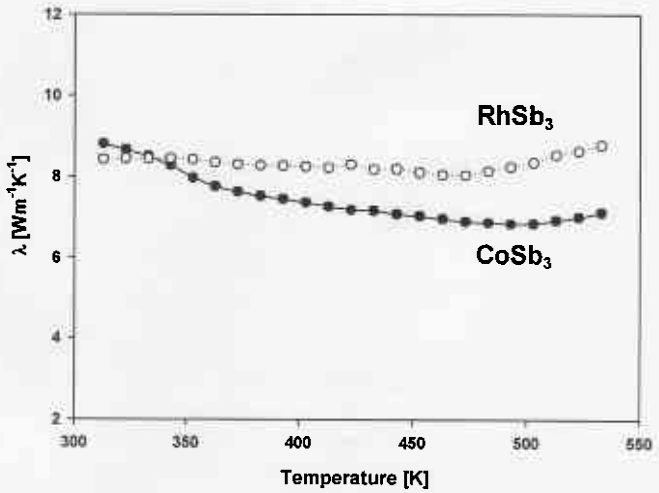

Fig. 4. Temperature dependence of the thermal conductivity λ for $CoSb_3$ and $RhSb_3$ samples. Estimated error of measurements 7%.

Theoretical study

The band structure of ordered $CoSb_3$ [13] and $RhSb_3$ was calculated by the fully charge self-consistent Korringa-Kohn-Rostoker method. The crystal potential of the muffin-tin form was constructed within the LDA framework using the von Barth-Hedin formula for the exchange-correlation part. The electronic structure of $Co_{1-x}Rh_xSb_3$ alloy was computed by the KKR method with the fully self-consistent coherent potential approximation (CPA) to treat a chemical disorder on transition metal site. The Fermi energy (E_F) was precisely determined from the generalised Lloyd formula [26,27]. For the final potentials (converged until mRy on the energy scale), total density of states (DOS), site-decomposed DOS and l-decomposed DOS (l_{max}=2) were calculated using k-space tetrahedron integration technique.

In the cubic body-centered skutterudite structure (Im3) Co (Rh) atoms and Sb atoms were located in the (8c) and (24g), respectively, while a large void was represented by an empty sphere in the (2a) site. All computations employed experimental values of lattice constant and atomic positions.

Electronic structure of $CoSb_3$ and $RhSb_3$

The band structure calculations using different methods already showed [7,9,13] that $CoSb_3$ is a narrow gap semiconductor. It was also noticed that the computed value of E_g is very sensitive to the choice of crystallographic (either experimental ones or these obtained from the total energy minimisation) and for example the energy gap obtained from the KKR method is as large as 70 meV whereas it was estimated of 0.22 eV in other study [28].

Although $RhSb_3$ compound is isoelectronic to $CoSb_3$, some modifications of electronic structure can be expected in the former due to unlike *d-p* hybridisation between *d*-states of transition metal (Co 3d shell versus Rh 4d shell) and *p*-states of Sb resulted in significantly larger interatomic distances in $RhSb_3$ with respect to $CoSb_3$.

Indeed, from the $E(\mathbf{k})$ dispersion curves computed in $RhSb_3$ one observes a small overlap among one valence band (non-degenerated in the whole BZ) and three conduction bands (degenerated depending on symmetry of k-points in BZ) at E_F, unlike the real energy gap found in $CoSb_3$.

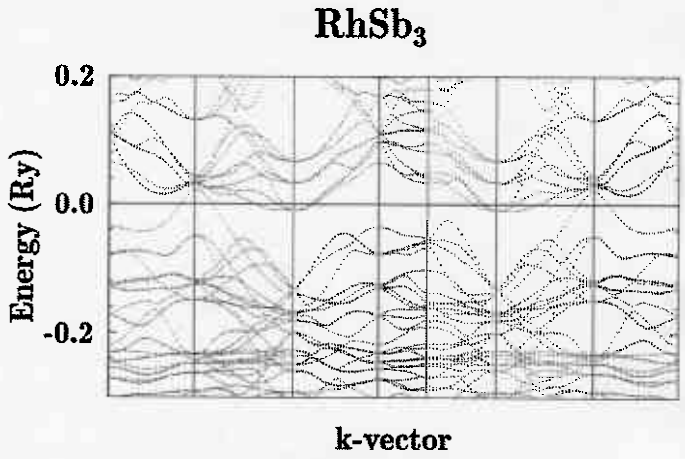

Fig. 5. Dispersion curves for $RhSb_3$

Interestingly, since the density of states at E_F does not vanish at E_F and the valence and conduction bands do not cross each other in the vicinity of the Fermi energy, we expect semimetallic properties of $RhSb_3$. Hence, comparing $E(\mathbf{k})$ curves in the parent compounds one can preview in $Co_{1-x}Rh_xSb_3$ alloy more or less systematic evolution of electronic structure from semiconducting-like (Co-rich compounds) to semimetallic-like (Rh-rich compounds) behaviours due to the band gap closing. These modifications of the Fermi surface topology in $Co_{1-x}Rh_xSb_3$ with Rh concentration should have an effect on type and transport parameters (e.g. effective masses) of conducting carriers. Furthermore, this is expected to be responsible for significant changes of electron transport properties versus alloy composition.

Electronic structure of $Co_{1-x}Rh_xSb_3$

KKR-CPA density of states in $Co_{0.75}Rh_{0.25}Sb_3$ and $Co_{0.75}Rh_{0.25}Sb_3$ compounds are presented in Fig. Xx. One can notice that with the Rh content the band gap closes (not easy to detect on KKR-CPA DOS) and the Fermi level shifts toward valence band. In $Co_{1-x}Rh_xSb_3$ the $N(E_F)$ value (in states/Ry) increases from zero (x=0) to 1.9 (x=0.25) and reaches 28 (x=0.5). Then, density of states at E_F slightly decreases to the 25 st/Ry for the x=1 sample. This result is well supported by the transition from semiconducting-like to semimetallic-like behaviour as seen on the temperature dependent resistivity curves.

The electronic structure changes in $Co_{1-x}Rh_xSb_3$ may suggest that rather complex conductivity mechanism responsible for transport behaviours. In Co-rich samples mostly electrons are dominated but in Rh-rich samples rather both types of carriers appear at the Fermi level (due to the valence and conduction band shift). From the curvature of these bands one can deduce that electrons should possess considerably heavier effective masses than holes (at least in

the semiconducting samples). This well corroborates with large and negative Seebeck coefficient observed in Co-rich samples (Fig. 3). Converesly, it is not evident to explain the positive value of the thermopower in Rh-rich compounds.

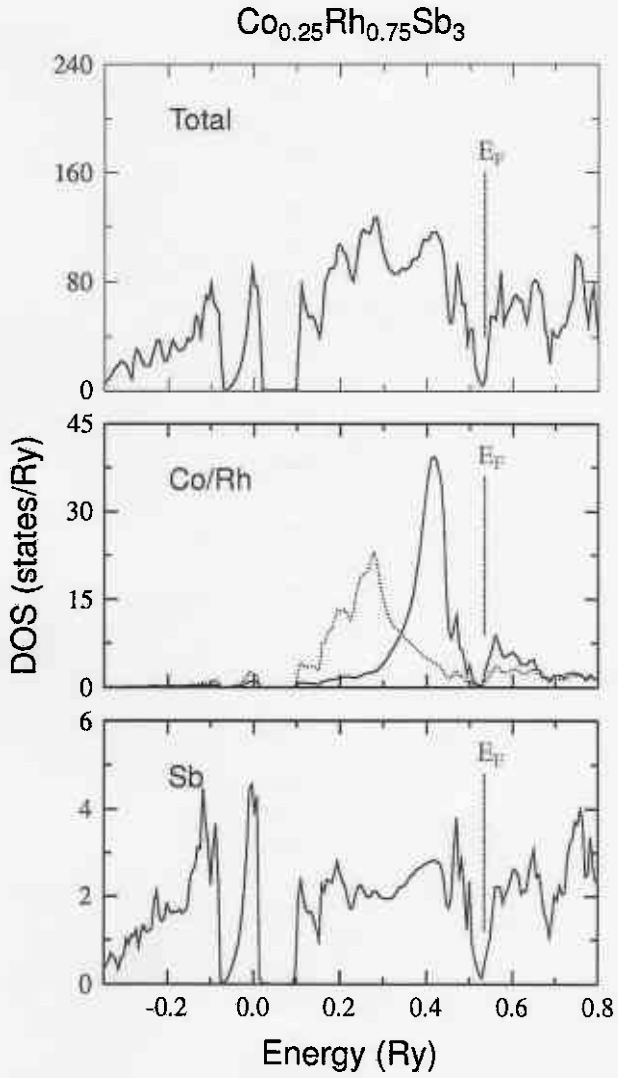

Fig. 6. KKR-CPA density of states in $Co_{0.25}Rh_{0.75}Sb_3$

Conclusions

Structural and physical properties of $CoSb_3$–$RhSb_3$ alloys were investigated in the whole range of composition. Despite of the lattice parameters generally follow Vegard's law, transport properties and some microstructural results seem to confirm that the miscibility gap exists in the range of x= 0.1 to 0.5 at low temperatures. However, both compounds can create full range solid solutions in high temperatures.

Alloying leads to the strong reduction of thermal conductivity about factor of 2 for composition of x = 0.27. Unfortunately, the reduction of thermal conductivity in this region is correlated with decrease of the electrical conductivity. In result, no enhancement in thermoelectric figure of merit is observed. On the other hand, n-type samples in this range of compositions exhibit semiconducting behaviour, quite large Seebeck coefficient and relatively low carrier concentration. It gives chances for further optimization of thermoelectric properties in order to receive higher ZT values.

The transition from semiconducting-like to semimetallic-like behaviour observed on resistivity curves in $Co_{1-x}Rh_xSb_3$ is well supported by the electronic structure KKR-CPA calculations. The effective masses of carriers estimated from the analysis of valence and conduction band curvature is comparable to the experimental data.

Acknowledgments

This work was supported by the State Committee for Scientific Research (KBN), grant No: 4 T08D 030 24.

References

1. Lutz HD, Kliche G. Lattice vibration spectra. XXVI. Far-infrared spectra of the ternary skutterudites $CoP_{3-x}As_x$, $CoAs_{3-x}Sb_x$, and $MGe_{1.5}Y_{1.5}$ (M=Co, Rh, Ir; Y=S, Se). *Journal of Solid State Chemistry, vol.40, no.1, Nov. 1981, pp.64-8.*
2. Shields V, Caillat T, Fleurial JP, Zoltan A, Zoltan L, Tuchscherer M. Synthesis and thermoelectric properties of $Co_{1-x}Ni_xP_3$ and $CoAs_{3-x}P_x$ skutterudites. *Proceedings ICT'02. 21st International Conference on Thermoelectrics (Cat. No.02TH8657). IEEE. 2002, pp.64-7. Piscataway, NJ, USA*
3. Watcharapasorn A, DeMattei RC, Feigelson RS, Caillat T, Borshchevsky A, Snyder GJ, Fleurial J-P. Thermoelectric properties of some cobalt phosphide-arsenide compounds. *Thermoelectric Materials 2000 - The Next Generation Materials for Small-Scale Refrigeration and Power Generation Applications (Materials Research Society Symposium Proceedings Vol.626). Mater. Res. Soc. 2001, pp.Z1.4.1-6. Warrendale, PA, USA.*
4. G.A. Slack, V.G. Tsoukala, some properties of semiconducting IrSb3, J. Appl. Phys. Vol. 76, 1665-1671 (1994).
5. Borshchevsky A, Fleurial J-P, Allevato E, Caillat T. $CoSb_3$–$IrSb_3$ solid solutions: preparation and characterization. *American Institute of Physics Conference Proceedings, no.316, 1995, pp.3-6.*
6. Caillat T, Borshchevsky A, Fleurial J-P. Existence and some properties of new ternary skutterudite phases. *American Institute of Physics Conference Proceedings, no.316, 1995, pp.209-11. USA..*
7. Sharp JW, Jones EC, Williams RK, Martin PM, Sales BC. Thermoelectric properties of $CoSb_3$ and related alloys. *Journal of Applied Physics, vol.78, no.2, 15 July 1995, pp.1013-18. USA*
8. Caillat T, Borshchevsky A, Fleurial J-P. Existence and some properties of new ternary skutterudite phases. *American Institute of Physics Conference Proceedings, no.316, 1995, pp.209-11. USA..*
9. Caillat T., Borshchevsky, and Fleurial J.-P., Properties of single crystalline semiconducting $CoSb_3$, J.Appl. Phys. 80 1996, pp 4442- 44449

10. Nolas G.S., Morelli T.D., Tritt T.M., Skutterudites: A phonon-Glass-Electron Crystall Approach to Advanced Thermoelectric Energy Conversion Applications, Annu. Rev. Mater. Sci. vol 29 (1999) pp 89-116
11. Ackermann J, Wold A. The preparation and characterization of the cobalt skutterudites CoP_3, $CoAs_3$ and $CoSb_3$. *Journal of Physics & Chemistry of Solids, vol.38, no.9, 1977, pp.1013-16.*
12. Ishii H, Okazaki K, Fujimori A, Nagamo Y, Koyanagi T, Sofo JO. Photoemission study of the skutterudite compounds $CoSb_3$ and $RhSb_3$ *Journal of the Physical Society of Japan, vol.71, no.9, Sept. 2002, pp.2271-5. Publisher: Phys. Soc. Japan, Japan*
13. Wojciechowski K.T, Toboła J., Leszczyński J., "Thermoelectric properties and electronic structure of $CoSb_3$ doped with Se and Te", J. Alloys Comp. **361** (1-2), 2003 pp. 19-27
14. Kurmaev E.Z., Moewes A., Shiein I.R., Finkelstein L.D., Ivanovskii A.L., and Anno H., Electronic structure and thermoelectric properties of skutterudite compounds, J. Phys.: Condens. Matter 16 (2004) pp. 979-987
15. Caillat T, Fleurial J-P, Borshchevsky A. Bridgman-solution crystal growth and characterization of the skutterudite compounds $CoSb_3$ and $RhSb_3$. *Elsevier. Journal of Crystal Growth, vol.166, no.1-4, 2 Sept. 1996, pp.722-6. Netherlands.*
16. Caillat T, Borshchevsky A, Fleurial J-P. Thermal expansion and some properties of $CoSb_3$, $RhSb_3$ and $IrSb_3$. *AIP. American Institute of Physics Conference Proceedings, no.301, pt.2, 1994, pp.517-20. USA*
17. Baoxing Chen, Jun-Hao Xu, Siqing Hu, Ctirad Uher. Thermoelectric properties of $RhSb_3$ crystals and thin films. *Advances in Microcrystalline and Nanocrystalline Semiconductors - 1996. Symposium. Mater. Res. Soc. 1997, pp.1037-42. Pittsburgh, PA, USA.*
18. Caillat T, Borshchevsky A, Fleurial J-P. Thermal expansion and some properties of $CoSb_3$, $RhSb_3$ and $IrSb_3$. *AIP. American Institute of Physics Conference Proceedings, no.301, pt.2, 1994, pp.517-20*
19. Kliche G, Bauhofer W. Infrared reflection spectra and electrical properties of the skutterudite $RhSb_3$. *Materials Research Bulletin, vol.22, no.4, April 1987, pp.551-5. USA.*
20. Takegahara K, Harima H. Systematic study of electronic band structures for binary skutterudite compounds. *Physica B, vol.328, no.1-2, April 2003, pp.74-6. Publisher: Elsevier, Netherlands.*
21. Sales B.C., Mandrus D., Chakoumakos B.C., Keppens V. and Thompson J.R., Filled skutterudite antimonides: Electron crystals and phonon glasses, *Phys. Rev. B, vol. 56, no 23, pp 15081-15089*
22. Anno H,. Matsubara K,. Caillat T., Fleurial J-P., Valence-band structure of the skutterudite compounds $CoAs_3$ $CoSb_3$ and $RhSb_3$ studied by X-ray photoelectron spectroscopy, Phys. Rev. B-Condensed Matter, vol.62, no.16, pp-10737-10743
23. Schmidt T., Kliche G., Lutz H.D. Structure refinement of skutterudite-type triantimonide, $CoSb_3$, Acta Cryst, 1987, C43, 1pp 678-1679
24. Rodriguez-Carvajal, J 1990 Satellite Mtg on Powder Diffraction of the 15th Congr. of the International Union of Crystallography (Toulouse, France) p 127
25. Fleurial J.P., Caillat, T. and Borshchevsky A., Skutterudites: An Update, Proc. of XVI Int. Conf. on Thermoelectrics, Dresden, Germany, August 26-29, 1997, IEEE Piscataway, NJ, p 1
26. Kaprzyk S. and Bansil A., Phys. Rev. B 42 (1990) 7358.
27. Bansil A., Kaprzyk S., Mijnarends P. E., Tobola J., Phys. Rev. B 60 (1999) 13396.
28. Sofo J.O. and Mahan G.D., Phys. Rev. 58 (1998) 15620.